Finite size scaling in asymmetric systems of percolating sticks

Milan Žeželj,* Igor Stanković, and Aleksandar Belić

Scientific Computing Laboratory, Institute of Physics Belgrade, University of Belgrade, 11080 Belgrade, Serbia

We investigate finite size scaling in percolating widthless stick systems with variable aspect ratios in an extensive Monte Carlo simulation study. A generalized scaling function is introduced to describe the scaling behavior of the percolation distribution moments and probability at the percolation threshold. We show that the prefactors in the generalized scaling function depend on the system aspect ratio and exhibit features that are generic to whole class of the percolating systems. In particular, we demonstrate existence of characteristic aspect ratio for which percolation probability at the threshold is scale invariant and definite parity of the prefactors in generalized scaling function for the first two percolation probability moments.

I. INTRODUCTION

Recently there is an increasing interest in the randomly distributed stick (rodlike) particles [1–5], due to promising developments in the area of the conducting rodlike nanoparticle networks, such as carbon nanotubes, silicon, copper, and silver nanowires, with applications in electronics [5–7], optoelectronics [8], and sensors [9, 10]. On the theoretical side, most of the work done until now in the field of percolation of random networks is done for lattice percolation [11–18]. The random stick networks are an important representative of continuum percolation [19–22]. Random stick percolation and lattice percolation fall into the same universality class having the same critical exponents [21]. Previous studies established that all systems fall on the same scaling function if dimensionality of the system, percolation rule, boundary conditions, and aspect ratio are fixed [15]. In applications, aspect ratio of the rectangular system is the only variable parameter, e.g., geometry of transistor gate channel in the carbon nanotube transistors [4, 5]. The objective of the present paper is to describe in consistent way finite size scaling of average percolation density and standard deviation for the asymmetric rectangular stick systems with free boundaries. From general scaling arguments one would expect that for all finite size systems their convergence is governed by an exponent $-1/\nu$ [18]. For two-dimensional (2D) systems $\nu = 4/3$ [18]. Following initial Ziff's publication [13], Hovi and Aharony [14, 15] argued that the irrelevant scaling variables in the renormalization-group treatment of percolation imply a slower leading-order convergence of percolation probability to its infinite-system value, characterized by an exponent $-1/\nu - \theta$, whose value was deducted from the Monte Carlo work of Stauffer to be $\theta \approx 0.85$ [11]. Further it was showed that for lattice percolation on the square system leading exponent of the average concentration at which percolation first occurs is $-1/\nu - \theta$, where $\theta \approx 0.9$ [17]. All the previous studies were performed for symmetric systems. We show that only in symmetric case the exponent of average density is $-1/\nu - \theta$. In asymmetric systems, we observe a leading $-1/\nu$ exponent. Another quantity, the percolation probability at the percolation threshold in

symmetric bond percolating systems is size independent, i.e., scale invariant [23]. Until now, this behavior is not observed in other types of random percolating systems. We will demonstrate that asymmetric systems can exhibit scale invariant behavior.

In this paper, we investigate finite size scaling of the asymmetric rectangular stick systems with free boundaries. Both from renormalization group considerations and in the simulations, we find that aspect ratio strongly influences scaling behavior of the percolation probability distribution function moments, i.e., average density of sticks at which percolation first occurs and variance of percolation probability distribution function. A generalized scaling function is introduced, with aspect ratio dependent prefactors and constant exponents of the expansion. Finally, it is shown that percolation probability of the asymmetric infinite sticks system at the critical threshold density agrees with Cardy's analytic formula [12].

II. NUMERICAL METHOD FOR CALCULATION OF PERCOLATION PROBABILITY

Monte Carlo simulations, coupled with an efficient cluster analysis algorithm and implemented on grid platform, are used to investigate the stick percolation [24–27]. We consider two dimensional (2D) systems with isotropically placed widthless sticks. The sticks of unit length are randomly positioned and oriented inside the rectangular system of width L_x and height L_y. Two sticks lie in the same cluster if they intersect. System percolates if two opposite boundaries are connected with the same cluster. The aspect ratio r is defined as the length of the rectangular system in percolating direction divided with the length in perpendicular direction. We define the normalized system size as a square root of the rectangular area $L = \sqrt{L_x L_y}$ (geometric average), which represent the length of the square system with the same area. The behavior of stick percolation is studied in terms of the number stick density $n = N/L^2$. The percolation threshold of infinite system is defined by the critical density $n_c \approx 5.63726$ [27]. Monte Carlo simulations are performed for wide range of the aspect ratios, $0.1 \leq r \leq 10$. In order to ensure the same precision for small and large systems we collected more than $N_{MC} = 10^9$ Monte Carlo realizations for small systems $L < 10$, down to $N_{MC} = 10^7$ for the largest system

$L = 320$. Using appropriate functions for fitting data and the least squares fitting methods excellent fits were obtained ($R^2 > 0.9999$) for all analyzed systems with $L \geq 16$. Statistical errors for the calculations are estimated in conventional fashion using standard deviation [24].

Percolation probability function $R_{N,L,r}$, is the probability that the system with N sticks, size L and aspect ratio r percolates. It is convenient to pass from the discrete percolation probability function $R_{N,L,r}$ for N sticks to a probability function for arbitrary stick density n [27]

$$R_{n,L,r} = \sum_{N=0}^{\infty} \frac{(nL^2)^N e^{-nL^2}}{N!} R_{N,L,r}, \qquad (1)$$

with percolation probability distribution function defined as $P_{n,L,r} = \partial R_{n,L,r}/\partial n$. The average stick percolation density at which, for the first time, a percolating cluster connects boundaries of the system is

$$\langle n \rangle_{L,r} = \int_0^{\infty} n P_{n,L,r} dn = \frac{1}{L^2} \sum_{N=0}^{\infty} (1 - R_{N,L,r}), \qquad (2)$$

where the last equality follows from integrating by parts. Another important parameter of probability distribution function, $P_{n,L,r}$, is variance $\Delta_{L,r}^2 = \langle n^2 \rangle_{L,r} - \langle n \rangle_{L,r}^2$, where $\langle n^2 \rangle_{L,r}$ is calculated as

$$\langle n^2 \rangle_{L,r} = \int_0^{\infty} n^2 P_{n,L,r} dn = \frac{2}{L^4} \sum_{N=0}^{\infty} (N+1)(1 - R_{N,L,r}). \qquad (3)$$

Equations (2) and (3) allow calculations of the first two moments directly from discrete percolation probability function $R_{N,L,r}$. This is computationally more efficient since it avoids calculation of function $R_{n,L,r}$ with high resolution.

III. GENERALIZED SCALING FUNCTIONS FOR MOMENTS

The percolation probability function is related to the universal scaling function [15]

$$R_{n,L,r} = F(\hat{x}, \{\hat{y}_i\}, \hat{z}). \qquad (4)$$

The arguments of the universal scaling function F are $\hat{x} = A(n - n_c)L^{1/\nu}$, $\hat{y}_i = B_i \omega_i L^{-\theta_i}$, and $\hat{z} = C \ln(r)$, where A, $\{B_i\}$, and C are the nonuniversal metric factors, $\{\omega_i\}$ are the irrelevant variables, and $\{\theta_i\}$ are the corrections to scaling exponents, ($i = 1, 2, ...$). Using free boundary conditions and considering two complementary systems: the sticks and empty space around the sticks, we can conclude that either the sticks percolate in one direction or the empty space percolates in the opposite direction:

$$F(\hat{x}, \{\hat{y}_i\}, \hat{z}) + F(-\hat{x}, \{-\hat{y}_i\}, -\hat{z}) = 1. \qquad (5)$$

Taking the derivative with respect to $\hat{x}$, $\hat{y}_i$, and $\hat{z}$ and evaluating the derivatives at $\hat{x} = \hat{y}_i = \hat{z} = 0$, (i.e., at $n = n_c, L \to \infty, r = 1$), we conclude that $\partial^m F / \partial \hat{x}^j \partial \hat{y}_1^{k_1} ... \partial \hat{z}^l \big|_0 = 0$, for

m even. Expanding the percolation probability function near the critical point we find that

$$F(\hat{x}, \{\hat{y}_i\}, \hat{z}) = F(0, \{0\}, 0) + f_0(\hat{x}, \hat{z}) + \sum_{i=1}^{\infty} f_i(\hat{x}, \hat{z})\hat{y}_i + ... \qquad (6)$$

where the functions $f_0(\hat{x}, \hat{z})$ and $f_i(\hat{x}, \hat{z})$ are defined by

$$f_0(\hat{x}, \hat{z}) = \sum_{j,l=0}^{\infty} \frac{1}{j!l!} \frac{\partial^{j+l} F}{\partial \hat{x}^j \partial \hat{z}^l} \bigg|_0 \hat{x}^j \hat{z}^l, \text{ for } j + l \text{ odd}, \qquad (7)$$

and

$$f_i(\hat{x}, \hat{z}) = \sum_{j,l=0}^{\infty} \frac{1}{j!l!} \frac{\partial^{j+l+1} F}{\partial \hat{x}^j \partial \hat{y}_i \partial \hat{z}^l} \bigg|_0 \hat{x}^j \hat{z}^l, \text{ for } j + l \text{ even.} \qquad (8)$$

Since percolation probability distribution function $P_{n,L,r} = \partial R_{n,L,r}/\partial n$ gives the probability distribution for a system of size L and aspect ratio r to percolate for the first time at stick density n, we can define the moments of this distribution

$$\mu_k = \int_0^{\infty} (n - n_c)^k \frac{\partial R_{n,L,r}}{\partial n} dn$$
$$= A^{-k} L^{-k/\nu} \int_{-An_c L^{1/\nu}}^{\infty} \hat{x}^k \frac{\partial F}{\partial \hat{x}} d\hat{x}, \qquad (9)$$

Substituting Eqs. (6)-(8) in Eq. (9) the kth moment scales as

$$\mu_k(\{\hat{y}_i\}, \hat{z}) = L^{-k/\nu} \left(g_0(\hat{z}) + \sum_{i=1}^{\infty} g_i(\hat{z})\hat{y}_i + ... \right), \qquad (10)$$

where we introduce general functions g. For odd k, $g_0(\hat{z})$ is odd function and $g_i(\hat{z})$ are even functions of $\hat{z}$. For even k, $g_0(\hat{z})$ is even and $g_i(\hat{z})$ are odd functions. Therefore, observed parity of prefactors in respect to $\hat{z}$ should be independent of the type of the system.

From Eq. (10) the scaling behavior of the $\langle n \rangle_{L,r}$ can be described with generalized moment scaling function with aspect ratio dependent coefficients

$$\langle n \rangle_{L,r} = n_c + L^{-1/\nu} \sum_{i=0}^{\infty} a_i(r) L^{-\theta_i}. \qquad (11)$$

where $\{\theta_i\}$ are the corrections to scaling exponents. The zeroth-order correction to exponent θ_0 should be zero [18]. In analogy to $\langle n \rangle_{L,r}$, for variance $\Delta_{L,r}^2$ we introduce expansion

$$\Delta_{L,r}^2 = L^{-2/\nu} \sum_{i=0}^{\infty} b_i(r) L^{-\theta_i}. \qquad (12)$$

From Eq. 10 and the parity of $g_0(\hat{z})$ and $g_i(\hat{z})$, for the zeroth-order and the first-order prefactors for $\langle n \rangle_{L,r}$ and $\Delta_{L,r}^2$ near $\ln(r) = 0$ (i.e., $\hat{z} = 0$), we obtain approximate expressions for $a_0(r) \approx a_{0,0} \ln(r) + a_{0,1} \ln^3(r)$, $a_1(r) \approx a_{1,0} + a_{1,1} \ln^2(r)$, $b_0(r) \approx b_{0,0} + b_{1,0} \ln^2(r)$, $b_1(r) \approx b_{1,0} \ln(r) + b_{1,1} \ln^3(r)$.

IV. RESULTS AND DISCUSSION

The results for percolation probability $R_{n,L,r}$ and distribution $P_{n,L,r}$ function are shown in Fig. 1. One observes that the slope of percolation probability function increases with the increase of the system size. The percolation probability function curves intersect approximately at n_c. The fine behavior of percolation probability at n_c will be discussed bellow. With the increasing system size, the standard deviation of probability distribution function decreases to zero. Also, average stick percolation density $\langle n \rangle_{L,r}$, which corresponds roughly to maximum of probability distribution function $P_{n,L,r}$, approaches to percolation threshold n_c. For $r < 1$, $\langle n \rangle_{L,r}$ converges to n_c from below with increase of the system size L. The reason for this is that narrow finite systems will be spanned already at lower densities than n_c. For $r > 1$, $\langle n \rangle_{L,r}$ converges from above, while for symmetric systems ($r = 1$) is roughly centered at n_c, see Fig 1. From Fig. 2, one can see that average stick percolation density $\langle n \rangle_{L,r}$ for aspect ratio higher than one is monotonically decreasing function of the system size L. Somewhat surprising, for aspect ratios lower than one, $\langle n \rangle_{L,r}$ is not monotonic function and has local minimum, i.e., for small systems $\langle n \rangle_{L,r}$ is a decreasing function, which passes through n_c, reaches a minimum and after that converges to n_c from below. In inset of Fig. 2, one can see that for large system sizes all the curves show power law convergence the percolation threshold n_c with exponent $-1/\nu$, except in the symmetric case, i.e., $r = 1$, where exponent is $-1/\nu - \theta_1$. Absolute values of the leading-order prefactors are the same for aspect ratios r and $1/r$. Higher exponent of symmetric systems comes from the basic physics of percolation that is connectedness. We can illustrate this using a simplified image of site percolation by introducing quantity $R(p)$ as probability that the sites with occupancy p form a spanning path. The percolation probability $R(p)$ and occupancy p are equivalent to the percolation probability function $R_{n,L,r}$ and stick density n, respectively. In this image, a cell coming out of the renormalization (coarse graining) transformation is occupied only if it contains a set of sites that span this cell. The universal scaling function in previous section reflects the fact that the probability of the spanning system at the percolation threshold $R(p_c)$ remains unaltered under this transformation [18]. Therefore fixed point of this system, i.e., the critical percolation threshold, p_c is satisfying relation $p_c = R(p_c)$. We can expand the percolation probability around the percolation threshold p_c, $|R(p) - R(p_c)| \approx dR/dp|_{p_c}|p - p_c|$. Also, if we renormalize lattice by a length factor b, close to p_c, characteristic length changes as ξ/b. Since $\xi \sim |p - p_c|^{-\gamma}$, we can write another relation, $|R(p) - R(p_c)|^{-\gamma} \approx |p - p_c|^{-\gamma}/b$, connecting characteristic lengths before and after renormalization. From these two relations one can conclude that critical exponent should be

$$-1/\gamma \approx \frac{\ln dR/dp|_{p_c}}{\ln 1/b}. \qquad (13)$$

From Fig 1, one can see that probability density $P_{n_c,L,r}$ which is derivative of $R_{n,L,r}$ at n_c, is always larger for symmetric systems than for asymmetric systems of the same size. There-

fore, from Eq. (13), one expects higher absolute value of the exponent in symmetric compared to asymmetric systems. Another conclusion one can draw from this analysis, is that the observed exponents are a result of the interplay of the characteristic length and the system shape. Usually, such behavior is attributed to a competition between two-dimensional and three-dimensional (or one-dimensional and two dimensional), e.g., in Ising model for slab geometries, cf. Ref [28]. In this system we observe that there is sharp transition in nature of scaling when we pass from symmetric to asymmetric system, and a competition between exponents characteristic for symmetric and asymmetric systems.
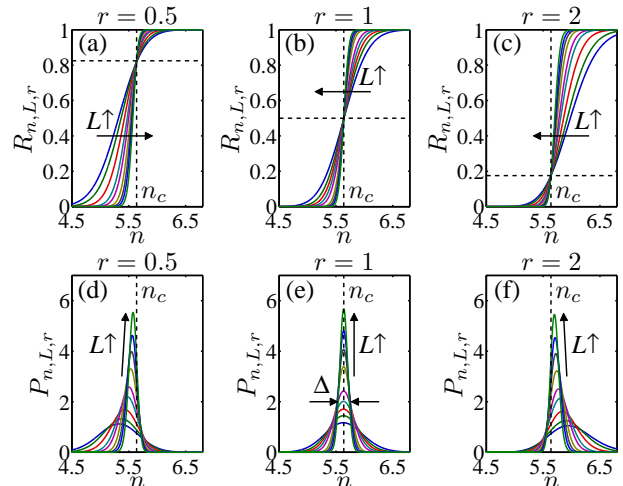

FIG. 1. (Color online) Percolation probability function $R_{n,L,r}$ (a, b, c) and probability distribution function $P_{n,L,r}$ (d, e, f) for stick percolation on rectangular systems with free boundary conditions and increasing system size from $L = 20$ to 200 for three aspect ratios $r = 0.5, 1$, and 2. The direction of the increase of L is indicated on graphs. The vertical dashed lines denote the value for the percolation threshold n_c, while the horizontal dashed lines (a, b, c) denote the percolation probability on the infinite systems at the threshold $R_{n_c,L \to \infty,r}$.

From Monte Carlo simulation data we have obtained the two leading-order terms of $\langle n \rangle_{L,r}$ in Eq. (11) by interpolation, cf. Ref. [29]. Results of the analysis are shown in Fig. 3. The zeroth-order prefactor is zero for symmetric system $r = 1$, and it is odd function on a logarithmic scale, i.e., $a_0(r) = -a_0(1/r)$. We have verified the obtained results by interpolation through symmetrizing data points $(\langle n \rangle_{L,r} + \langle n \rangle_{L,1/r})/2$. The fitting coefficients for prefactors $a_{i,j}$ are calculated using the least squares fitting methods and given in Table I, cf. Fig. 3. Influence of higher order terms were comparable or smaller than simulation data error and we could not extract them with sufficient precision. For the first-order correction, we obtain $\theta_1 = 0.83(2)$ for $r = 1$, cf. Ref. [11, 13]. The residual aspect ratio dependence of θ_1 cannot be further analyzed without provision of retaining the first two terms in Eq. (11). The system size where the average density reaches minimum is $L_{\min} \approx (-a_1(r)/a_0(r)(1 + \nu\theta_1))^{1/\theta_1}$, cf. Eq. (11). For narrow systems, $r < 1$, $L_{\min}$ diverges as $1/\ln(r)$ as r approaches one. For $L < L_{\min}$ the first-order term is dominant.
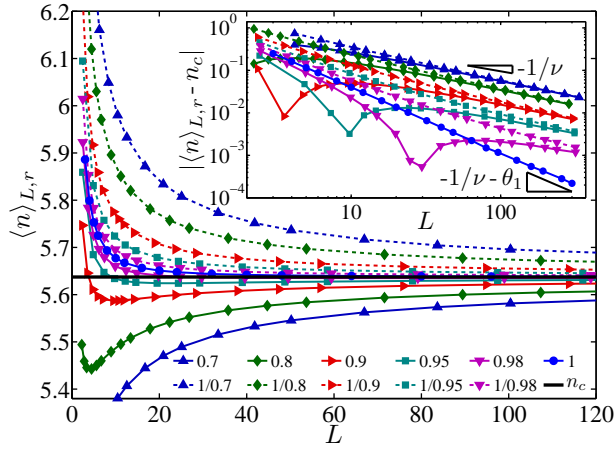
FIG. 2. (Color online) The dependence of the average stick percolation density $\langle n \rangle_{L,r}$ on the system size L and aspect ratio r. The values are obtained from Monte Carlo simulations and calculated using Eq. (2). The values are given for aspect ratios $r = 0.7, 0.8, 0.9, 0.95, 0.98, 1$ (solid lines) and their inverse values $r = 1/0.7, 1/0.8, 1/0.9, 1/0.95, 1/0.98$ (dashed lines). The horizontal bold line denotes the expected value for the percolation threshold n_c. Inset: The same data is shown in logarithmic scale to demonstrate the same power law convergence of the r and $1/r$ pairs.
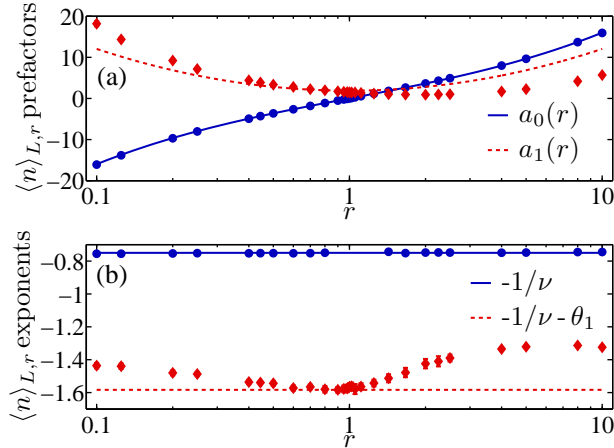

FIG. 3. (Color online) Prefactors (a) and exponents (b) are shown for the two leading-order terms of generalized scaling function for average stick percolation density $\langle n \rangle_{L,r}$, Eq. (11). The zeroth-order prefactor is odd function on a logarithmic scale, i.e., $a_0(r) = -a_0(1/r)$, and the zeroth-order exponent is $-1/\nu$ (solid lines). The first-order prefactor is even function, i.e., $a_1(r) = a_1(1/r)$ and the first-order correction to the scaling exponent is $\theta_1 = 0.83(2)$ for $r = 1$ (dashed lines).

The variance prefactors and exponents for the two leading-order terms are shown in Fig. 4. The prefactors and exponents are obtained by fitting $\Delta_{L,r}^2$ with the first two terms in Eq. (12), cf. Ref. [30]. The fitting coefficients $b_{i,j}$ are given in Table I and obtained prefactor dependences on r are given in Fig. 4. The zeroth-order prefactor of $\Delta_{L,r}^2$ is even function on a logarithmic scale, i.e., $b_0(r) = b_0(1/r)$, as one can see

TABLE I. Results for the coefficients $a_{i,j}$ and $b_{i,j}$, where $i,j \in \{0,1\}$. The results are obtained using the least squares method.

	0, 0	0, 1	1, 0	1, 1
$a_{i,j}$	5.08(1)	0.352(4)	1.9(5)	1.9(6)
$b_{i,j}$	14.56(5)	2.25(6)	11(2)	3(1)

from a coarse observation of the percolation probability distribution function in Fig. 1. Asymmetry of the variance, i.e. $\Delta_{L,r}^2 \neq \Delta_{L,1/r}^2$, is the first-order effect, cf. Eq. (12).
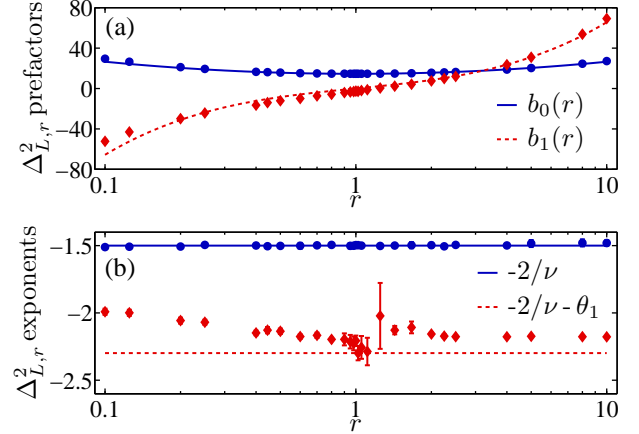

FIG. 4. (Color online) Prefactors (a) and exponents (b) are shown for the two leading-order terms of generalized scaling function for variance $\Delta_{L,r}^2$, Eq. (12). The zeroth-order prefactor is even function on a logarithmic scale, i.e., $b_0(r) = b_0(1/r)$ and the zeroth-order exponent is $-1/\nu$ (solid lines). The first-order prefactor is odd function, i.e., $b_1(r) = -b_1(1/r)$, and the first-order correction to the scaling exponent is $\theta_1 = 0.80(5)$ for $r = 1$ (dashed lines). Prefactor $b_1(r)$ passes through zero for r between $1/0.9$ and $1/0.8$ causing higher error bars of θ_1.

Finally, we investigate scaling behavior of percolation probability at the percolation threshold ($R_{n_c,L,r}$), using the generalized scaling function $R_{n_c,L,r} = R_{n_c,L\to\infty,r} + c_1(r)/L + c_2(r)/L^2$, cf. Ref. [17]. The results for prefactors $c_1(r)$ and $c_2(r)$ are shown in Fig. 5. For two limiting cases ($r < 0.1$ and $r > 10$), the prefactors are close to zero, what is consistent with behavior observed in Fig. 1. Between these two limiting cases, one can observe that both prefactors are close to zero for $r = 2.25(5)$. Furthermore, at this aspect ratio, we could not observe existence of the higher order terms. This means that at the percolation threshold percolation probability is the same for all the systems, independent of system size L, having the value $R_{n_c,r\approx2.25} \approx 0.135$. Scale invariance, i.e., $R_{n_c,L,r} = R_{n_c,\infty,r}$ is already seen and intuitively understood for bond percolation in symmetric systems, where $R_{p_c=0.5,r=1} = 1/2$ is independent of system size L, cf. Ref. [23]. The reason for observed system size invariance of percolation probability at the threshold in the asymmetric stick system is existence of multiple zero of at least second order at this point in universal scaling function. Regarding value of percolation probability at the percolation threshold of infinite system, we find that Cardy's analytical model de-

rived for the lattice percolation describes simulation data, cf. Fig. 5. The deviation between analytical value for lattice and Monte Carlo value for stick percolation is less than statistical error of the simulation data, i.e., less than 10^{-5}. Percolation probability for 2D sticks system therefore satisfies $R_{n_c,L\to\infty,r} + R_{n_c,L\to\infty,1/r} = 1$.

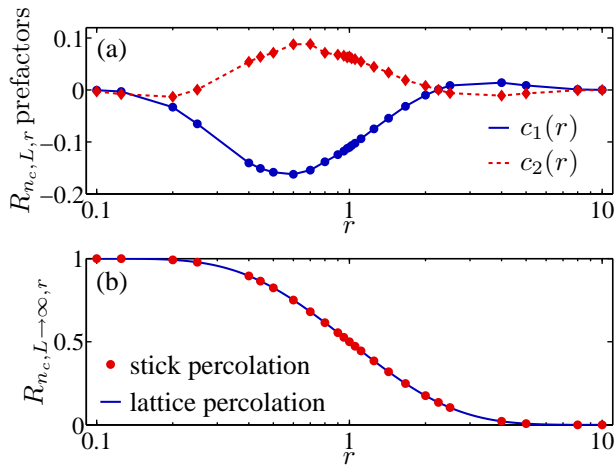FIG. 5. (Color online) (a) Prefactors for finite size scaling of the percolation probability at the percolation threshold are shown for the two leading-order terms. (b) Percolation probability at the threshold for infinitely large system $R_{n_c,L\to\infty,r}$. Points represent Monte Carlo data for stick percolation, while line represents results of Cardy's model for the lattice percolation. The error bars are much smaller than the size of the symbols for all r

V. CONCLUSION

In summary, based on the analysis of finite size scaling in continuum two-dimensional systems, the generalized scaling law is introduced for average percolation density, variance, and percolation probability at the percolation threshold. The

presented methodology could be used to model accurately these properties for any percolating system. We find that the zeroth-order prefactor of average percolation density is odd function with respect to $\ln(r)$. This explains the faster convergence of average percolation density for symmetric systems than expected from general scaling arguments. We also observe that there is a characteristic aspect ratio for which percolation probability at the percolation threshold is system size independent. In addition, for infinite system, we find that percolation probability at the critical threshold density shows excellent agreement with the Cardy's prediction for lattice percolation. The presented results confirm that continuum percolation belongs to the same universality class as lattice percolation in the sense that value of percolation probability at the threshold for infinitely large systems is the same for lattice and continuum percolation. One should note that a number of other features observed in this work should be a common characteristic within the class, e.g., existence of the aspect ratio where the percolation probability at the threshold is scale invariant and parity of the moments of the percolation probability distribution function. This opens up the question of the particle shape influence on prefactors, weather it is possible to find systems where the observed behaviors are more pronounced, and finally the question of the general form of the prefactors for describing different systems.

[1] R. Ramasubramaniam, J. Chen, and H. Liu, Appl. Phys. Lett. **83**, 2928 (2003).

[2] A. Trionfi, D. H. Wang, J. D. Jacobs, L.-S.Tan, R. A. Vaia, and J. W. P. Hsu, Phys. Rev. Lett. **102**, 116601 (2009).

[3] Y. Hazama, N. Ainoya, J. Nakamura, and A. Natori, Phys. Rev. B **82**, 045204 (2010).

[4] X.-Z. Bo, N. G. Tassi, C. Y. Lee, M. S. Strano, C. Nuckolls, G. B. Blanchet, Appl. Phys. Lett. **87**, 203510 (2005).

[5] V. K. Sangwan, A. Behnam, V. W. Ballarotto, M. S. Fuhrer, A. Ural, and E. D. Wiliams, Appl. Phys. Lett. **97**, 043111 (2010).

[6] J. Li, Z.-B. Zhang, M. Östling, S.-L. Zhang, Appl. Phys. Lett. **92**, 133103 (2008).

[7] S. Kumar, J.Y. Murthy, and M. A. Alam, Phys. Rev. Lett. **95**, 066802 (2005).

[8] L. Hu, D. S. Hecht, and G. Grüner, Nano Lett. **4**, 2513 (2004).

[9] Q. Cao, H.-S. Kim, N. Pimparkar, J. P. K., C. W., M. Shim, K. Roy, M. A. Alam, and J. A. Rogers, Nature **454**, 495 (2008).

[10] J. Li and S.-L. Zhang, Phys. Rev. B **79**, 155434 (2009).

[11] D. Stauffer, Phys. Lett. A **83**, 404 (1981).

[12] J. L. Cardy, J. Phys. A **25**, L201 (1992).

[13] R. M. Ziff, Phys. Rev. Lett. **. 69**, 2670 (1992).

[14] A. Aharony and J.-P. Hovi, Phys. Rev. Lett. **. 72**, 1941 (1994).

[15] J.-P Hovi and A. Aharony, Phys. Rev. E **53**, 235 (1996).

[16] M. E. J. Newman and R. M. Ziff, Phys. Rev. Lett. **. 85**, 4104 (2000).

[17] R. M. Ziff and M. E. J. Newman, Phys. Rev. E 66, 016129 (2002).

[18] D. Stauffer and A. Aharony, *Introduction to Percolation Theory*, 2nd revised ed. (Taylor and Francis, London, 2003).

[19] G. E. Pike and C. H. Seager, Phys. Rev. B **10**, 1421 (1974).

[20] I. Balberg and N. Binenbaum, Phys. Rev. B **28**, 3799 (1983).

[21] I. Balberg, N. Binenbaum, and C. H. Anderson, Phys. Rev. Lett. **51**, 1605 (1983).

[22] I. Balberg, C. H. Anderson, S Alexander, and N. Wagner, Phys. Rev. B **30**, 3933 (1984).

[23] J. Bernasconi, Phys. Rev. B **18** 2185 (1978).

[24] M. E. J. Newman and R. M. Ziff, Phys. Rev. E . **64**, 016706 (2001).

[25] I. Stanković, M. Kröger and S. Hess, Comp. Physics Comm. **145**, 371 (2002)

[26] A. Balaž, O. Prnjat, D. Vudragović, V. Slavnić, I. Liabotis, E. Atanassov, B. Jakimovski and M. Savić, J. Grid. Comput. **9**, 135 (2011).

[27] J. Li and S.-L. Zhang, Phys. Rev. E . **80**, 040104 (2009).

[28] M. Plischke and B. Bergersen, *Equilibrium Statistical Physics*, 3rd ed., (World Scientific, Singapore, 2005).

[29] In order to obtain θ_0 with high precision successive slopes between points L and $L/2$ [17] are calculated. The slope is defined as $(\ln|\langle n\rangle_{L,r} - n_c| - \ln|\langle n\rangle_{L/2,r} - n_c|)/\ln 2$. This is approximately $(a_1(r)/a_0(r)/\ln 2)(1 - 2^{\theta_1 - \theta_0})L^{-\theta_1 + \theta_0} - 1/\nu - \theta_0$ when $|a_0(r)| \gg |a_1(r)|L^{-\theta_1 + \theta_0}$. Therefore, successive slopes should fall on a straight line when plotted as a function of $L^{-\theta_1 + \theta_0}$ with intercept at $-1/\nu - \theta_0$. The intercept is not highly sensitive to the value of $-\theta_1 + \theta_0$. Note that exponent θ_0 can not be calculated using successive slopes if $a_0(r)$ is close to zero.

[30] The zeroth-order exponent for $\Delta^2_{L,r}$ can be calculated using successive slopes for all r because condition $|b_0(r)| \gg |b_1(r)|L^{-\theta_1 + \theta_0}$ is always satisfied. The results for the zeroth-order terms are verified by interpolation through anti-symmetrizing data points $(\Delta^2_{L,r} - \Delta^2_{L,1/r})/2$.